Materials Science and Engineering C 61 (2016) 688–694

Contents lists available at ScienceDirect

Materials Science and Engineering C

journal homepage: www.elsevier.com/locate/msec

Submicron magnetic core conducting polypyrrole polymer shell: Preparation and characterization

Ernandes Taveira Tenório-Neto [a,c], Abdoullatif Baraket [b], Dounia Kabbaj [d], Nadia Zine [b], Abdelhamid Errachid [b], Hatem Fessi [a], Marcos Hiroiuqui Kunita [c], Abdelhamid Elaissari [a,*]

[a] University of Lyon, F-69622, Lyon, France, University Lyon-1, Villeurbanne, CNRS, UMR-5007, LAGEP-CPE, 43 Bd 11 Novembre 1918, F-69622 Villeurbanne, France
[b] Institut des Sciences Analytiques (ISA), Université Lyon, Université Claude Bernard Lyon-1, UMR-5180, 5 Rue de la Doua, F-69100 Villeurbanne, France
[c] State University of Maringá, Department of Chemistry, Av. Colombo, 5790, CEP 87020-900 Maringá, Paraná, Brazil
[d] Universiapolis, International University of Agadir, Technopole Agadir, Bab El Madina, 80000 Agadir, Morocco

ARTICLE INFO

Article history:
Received 9 November 2015
Received in revised form 14 December 2015
Accepted 23 December 2015
Available online 29 December 2015

Keywords:
Magnetic latex particles
Magnetic emulsion
Seed polymerization
Encapsulation
Functionalization

ABSTRACT

Magnetic particles are of great interest in various biomedical applications, such as, sample preparation, in vitro biomedical diagnosis, and both in vivo diagnosis and therapy. For in vitro applications and especially in labs-on-a-chip, microfluidics, microsystems, or biosensors, the needed magnetic dispersion should answer various criteria, for instance, submicron size in order to avoid a rapid sedimentation rate, fast separations under an applied magnetic field, and appreciable colloidal stability (stable dispersion under shearing process). Then, the aim of this work was to prepare highly magnetic particles with a magnetic core and conducting polymer shell particles in order to be used not only as a carrier, but also for the in vitro detection step. The prepared magnetic seed dispersions were functionalized using pyrrole and pyrrole-2-carboxylic acid. The obtained core–shell particles were characterized in terms of particle size, size distribution, magnetization properties, FTIR analysis, surface morphology, chemical composition, and finally, the conducting property of those particles were evaluated by cyclic voltammetry. The obtained functional submicron highly magnetic particles are found to be conducting material bearing function carboxylic group on the surface. These promising conducting magnetic particles can be used for both transport and lab-on-a-chip detection.

1. Introduction

Conducting polymers (CPs) are carbon-based molecules, which exhibit electrical, optical, and electronic properties analogous to metals. However, if compared to metals, CPs have advantages due to their polymer properties, such as, flexibility, low toxicity, low cost, and easy processing [1]. All these characteristics make CPs a potential material for applications in sensors, fuel cells, energy storage, and so forth [2]. In sensors, the charge transport properties of conducting polymers are changed when exposed to some analytes. This change in transport charge can be correlated directly to the concentration of target analyte [3].

Polyaniline (PANI), polypyrrole (PPy), polythiophene, and their derivatives are a class of CPs which are most studied specially due to their facile synthesis and flexibility in processing [2]. In addition, their conductivity ranges from 10^{-10} S cm^{-1} to 10^{-5} S cm^{-1} [4]. Among CPs, polypyrrole is one of the most extensively used in conducting polymers for the construction of bioanalytical sensors and supporting matrix in electrochemicals due to its good physical and electrical properties, high conductivity, chemical stability, and biocompatibility [5–7]. CPs containing specific functional groups can exhibit individual physicochemical properties if compared to the original polymer. For example, carboxylic acid-functionalized CPs can be used for DNA, proteins, and enzyme immobilization [8,9].

Magnetic latex (ML) particles have attracted much attention due to their properties, especially superparamagnetism, which makes them responsive to an external magnetic field. This unique property has been exploited in fast separation applications and particularly the in vitro biomedical diagnostic domain. In this sense, superparamagnetic nanoparticles have been used in core–shell structures for improving chemical stability of the magnetic core, while the shell can be tuned providing functional groups for specific interactions and applications.

Combining both electrical and magnetic properties in one particle is of paramount importance in order to be used as a carrier and for detection in a sensor field or in any microsystem based on microfluidics. Different approaches have been described to prepare magnetic latex particles. These approaches are based on classical polymerization in dispersed media, such as, emulsion [10], suspension [11], miniemulsion [12], dispersion [13], combination of various polymer-based process [14], and inverse emulsion [15]. The pioneer work was reported by Ugelstad et al. [16] by performing micron magnetic particles in more than two steps. Two of the magnetic latex particles were prepared;

* Corresponding author.
E-mail address: Elaissari@lagep.univ-lyon1.fr (A. Elaissari).

http://dx.doi.org/10.1016/j.msec.2015.12.052
0928-4931/

2.8 μm and 4.2 μm size with high sedimentation velocity. On the other hand, Elaissari et al. [17] have reported the synthesis of magnetic latexes using a process called seeded emulsion polymerization. This process leads to submicron ML particles containing high iron oxide content. These prepared functional, submicron, and highly magnetic particles have been used for nucleic acid extraction and purification [18], capturing of analyte in biological samples [19], controlling protein adsorption and desorption as a function of numerous parameters [20], in vivo molecular imaging [21], and in immunodiagnostics for specific antigen detection [22].

In order to take advantage of conductive properties from polypyrrole-coated latexes and to improve by that way the accuracy of the biosensing event, in this work, we describe the preparation, and characterization of polypyrrole-coated magnetic particles. To prepare such material, a seeded emulsion polymerization process was used. For obtaining magnetic responsive particles, magnetic emulsion (ME), containing superparamagnetic iron oxide nanoparticles, was used as the seed. In order to obtain acid-functionalized CPs on the particle surface, pyrrole (Py) was copolymerized with pyrrole-2-carboxylic acid (Py-2-COOH). The obtained core–shell magnetic particles were characterized in terms of particle size, size distribution, FTIR analysis, morphology, chemical composition, and finally, both magnetic and electric behaviors were studied. Moreover, the influence of monomer composition on the final morphology was also investigated.

2. Experiments

2.1. Materials

Pyrrole (Py) 98%, povidone (PVP), pyrrole-2-carboxylic acid (Py-2-COOH) 99%, and iron chloride hexahydrate 97% ($FeCl_3 \cdot 6H_2O$) were purchased from Sigma-Aldrich. The oil-in-water magnetic emulsion (ME) (total solid content 7.9%) consisted of magnetite nanoparticles stabilized with oleic acid, octane, and dodecyl sodium sulfate was acquired from Ademtech S. A. (lot E5 255b-2). Pyrrole was purified by passing through a column of activated basic alumina (Acros) before use. All other reagents were used without further purification and aqueous solutions were prepared with deionized water.

2.2. Synthesis of magnetic particle-coated Py/Py-2-COOH

The seeded-polymerization was carried out in a 25 mL glass reactor using a Teflon paddle stirrer. For each experiment, 1.52 g of magnetic emulsion (ME) (0.12 g dried extract) was weighed, and added into the reactor. Then, the supernatant was removed after 5 min of magnetic separation. After that, 10 mL of aqueous solution containing PVP (stabilizing agent) was added into the reactor and ME was redispersed under continuous stirring (300 rpm) for 4 h. Then, desired amounts of Py and Py-2-COOH (monomers) were added into the reactor (see Table 1) with 90 mg $FeCl_3 \cdot 6H_2O$ (initiator). The reaction was kept under stirring during 12 h at room temperature.

Table 1
Compositions of monomers (Py and Py-2-COOH) and stabilizer (PVP) employed during seeded polymerization.*

Sample name	Py (mmol)	Py-2-COOH (mmol)	PVP (mg)
1600	16	00	20
1608	16	08	20
1616	16	16	20
1632	16	32	20
3232	32	32	20
1616-PVP0	16	16	00
1616-PVP5	16	16	05
1616-PVP10	16	16	10

* 90 mg $FeCl_3 \cdot 6H_2O$, RT, 12 h.

3. Characterization

3.1. Transmission electron microscopy

Transmission electron microscopy, TEM, was performed with a Philips CM120 microscope at the "Centre Technologique des Microstructures" (CTμ) at the University of Lyon (Villeurbanne, France). Briefly, a drop of sample diluted in distilled water was deposited on a carbon-coated copper grid and then left to dry, at room temperature, overnight before TEM imaging.

3.2. Particle size measurements

A Malvern Zetasizer (Nano ZS, Malvern Instruments Limited, UK) was used to measure the average hydrodynamic size (D_h) of the magnetic polymer colloidal particles in 10^{-3} mol L^{-1} NaCl solution. The average of at least five measurements (10 runs for each colloidal dispersion) was taken into consideration.

3.3. Fourier transformed infrared (FTIR)

The investigation of surface properties of the obtained sample was performed using attenuated total reflection–Fourier transformed infrared spectrophotometer (ATR–FTIR — Shimadzu, Japan. All samples were clean and dry before analysis. The spectra were scanned over range 4000–400 cm^{-1}.

3.4. Zeta potential measurements

Malvern Zetasizer (Nano ZS, Malvern Instruments limited, UK) was used to measure the electrophoretic mobility, which is converted to Smoluchowski's zeta potential. The measurements were performed using a highly diluted dispersion of the considered colloidal particles in 10^{-3} mol L^{-1} NaCl solution at different pH. The pH was adjusted using NaOH or HCl. Each recorded value was the average of three measurements.

3.5. Thermal gravimetric analysis (TGA)

Thermo-gravimetric analysis measurements were carried out on a thermogravimetry analyzer (NETZSCH-TG209F1 Iris®ASC). The measurements were performed under a N_2 atmosphere from ambient temperature up to 1000 °C at a heating rate of 10 °C min^{-1}. Before analysis, the magnetic core–shell particles were separated from their supernatant by applying a permanent magnetic field and then washed with deionized water. This procedure was done in order to remove the non-magnetic material such as surfactant and free polymer particles. After that, the samples were dried at 40 °C for 24 h before analysis.

3.6. Magnetic properties

The saturation magnetization and magnetic behavior of the dried magnetic polymer latexes were investigated using a vibrating sample magnetometer. Magnetization measurements were carried out at room temperature on the automatic bench of magnetic measurements at CNRS-IRC Lyon.

3.7. Cyclic voltammetry (CV) and impedance measurements (EIS)

Electrochemical characterizations were carried out by using a VMP-3 potentiostat (Biologic CE-Lab VMP3). All measurements for CV and EIS analysis were made at room temperature (approx. 24 °C). The electrolyte for both CV and EIS measurements was made from a redox probe using ferro- and ferricyanide $K_3(Fe(CN)_6)/K_4(Fe(CN)_6)$ at 5 mM in PBS buffer (pH 7.4). Electrochemical measurements were made within a teflon cell in which the gold working electrode (WE) was sandwiched

between the two parts of the electrochemical cell (see Supplementary data). Platinum wire was used as the counter electrode (CE) and a calomel saturated electrode was used as the reference electrode (RE). The gold area exposed to the electrolyte was approx. 3 mm in diameter. The volume of ferrocyanide buffer was affixed for all measurements at 1.3 mL.

4. Results and discussions

4.1. Influence of monomer composition on the morphology

Fig. 1 shows TEM images of final magnetic particles prepared using different amounts of Py and Py-2-COOH. Polymerizations were conducted using magnetic emulsion (ME) as the seed. During polymerization, the monomers are oxidized under the action of Fe^{3+} ions. This leads to the formation of radical cations of Py/Py-2-COOH, which connect either to monomers/oligomers or polymer chains already synthesized [23].

As shown in Fig. 1A ME exhibits a spherical shape with a narrowed size distribution. After polymerization using pyrrole, sample 1600 (Fig. 1B), a thin and smoothed layer of conducting polymer covering the ME surface was clearly evidenced. The effect of monomer composition on the morphology can be explained in terms of polymer solubility. Polypyrrole (PPy) exhibits poor solubility in water [6], for this reason, polypyrrole has more affinity to the ME surface (which is hydrophobic). During polymerization PPy spreads on the ME surface covering particle surface by a uniform way leading to a smoothed coating. However, when the Py-2-COOH was added to the formulation (Fig. 1C to F), core–shells were obtained with a roughness surface. Py-2-COOH has carboxyl groups and when its amount is increased in the polymerization recipe, the formed polymer become more hydrophilic. Consequently, the efficiency on the covering ME surface decreases leading to a rough surface.

4.2. Influence of stabilizer on the morphology

The influence of the PVP amount on the final particle morphology was also investigated. For performing these experiments, sample 1616 was chosen for the comparison rate related to Py and Py-2-COOH. Fig. 2A shows the TEM images of sample 1616 synthesized without a stabilizer. It can be seen in this figure that a perfect homogeneous shell could be obtained, but all prepared particles were aggregated and could not be redispersed even using ultrasound. When 5 mg of stabilizer was added to the sample composition, the cluster amount decreased. The same behavior was observed when the PVP amount was 10 mg. However, good dispersion was only obtained when the PVP amount reached 20 mg (see Fig. 1D).

4.3. FTIR results

Fig. 3 shows the FTIR spectra of magnetic emulsion (ME), 1600, and 1632 in the spectral range of 2000 cm^{-1} to 800 cm^{-1}. ME was prepared by emulsification of ferrofluid (oil phase) in water solution containing surfactant. Besides that, in the oil phase, iron oxide particles are stabilized with oleic acid (OA). In ME spectra, it could be observed as an absorption band near 1700 cm^{-1} which is ascribed to C=O stretching of free OA [24,25]. However, for sample 1600, the same one was shifted near 1660 cm^{-1} probably due to interactions between free oleic acid with polypyrrole chains.

On the other hand, for sample 1632, the peak near 1660 cm^{-1} could also be attributed to C=O stretching ($\nu_{C=O}$) from Py-2-COOH segments. The reduction of carbonyl stretching frequencies is associated with two factors: i) The molecule of Pyrrole-2-carboxylic acid has unsaturation in the α,β-position which is conjugated with carboxylic groups. ii) Due interaction by hydrogen bonds, dimers can be formed [26]. Dubis et al. have investigated vibrational models of Py-2-COOH by FTIR and Raman [27]. They found that the Py-2-COOH molecule contains O–H,

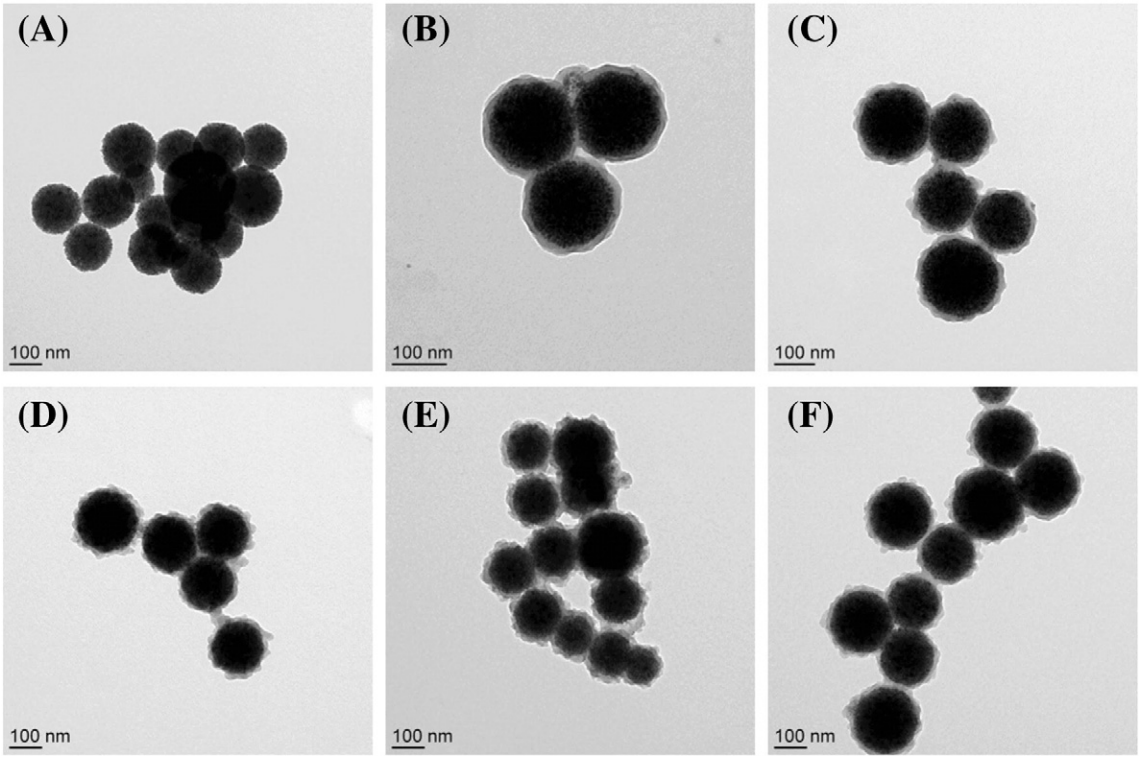

Fig. 1. TEM images for samples obtained by seeded-polymerization changing the monomer composition: (A) Magnetic emulsion, (B) 1600, (C) 1608, (D) 1616, (E) 1632, and (F) 3232.

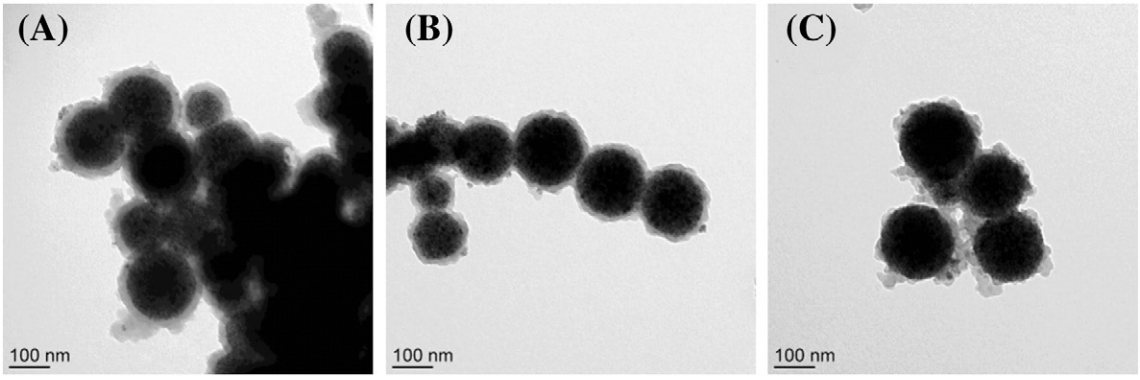

Fig. 2. TEM images for samples obtained by seeded-polymerization changing the amount of stabilizer: (A) 1616-PVP0, (B) 1616-PVP5, and (C) 1616-PVP10.

C=O, and N–H groups which may generate different types of hydrogen-bonded dimers linked either through R–C=O···H–O–R′ or R–C=O···H–N–R′ groups. Thus, the absorption band of C=O stretching of Py-2-COOH can be found between 1685 cm^{-1} and 1660 cm^{-1} overlapping the same $\nu_{C=O}$ absorption band of OA.

The high-intensity band near 570 cm^{-1}, corresponding to Fe–O stretching vibration, was observed in all samples indicating the presence of the magnetic phase in polymer particles [5,23]. In addition, peaks at 1547 cm^{-1} and 1037 cm^{-1} were attributed, respectively, to C=C stretching and =C–H in plane bending vibration from poly(pyrrole-co-pyrrole-2-carboxylic acid) rings; the peak at 1170 cm^{-1} was ascribed to C–N stretching vibration [2,28]. While the signal at 911 cm^{-1} was attributed to =C–H out-of-plane bending vibration [29].

4.4. Thermogravimetric analysis

Fig. 4A shows the thermogram of ME used as the seed during polymerization. These experiments were carried out under N_2 atmosphere. In this figure, it can be visualized that degradation of magnetic emulsion could be divided into three steps: (i) 25–500 °C, (ii) 501–850 °C, and (iii) above 850 °C. The first step is associated with degradation of the organic part (approx. 20%), which corresponds to the used oleic acid surfactants in ME preparation. The second step is attributed to the phase transition from Fe_3O_4 to FeO (weight loss approx. 2.5%), because FeO is thermodynamically stable above 570 °C [30]. The third one is attributed to reduction of FeO. In this case, FeO is totally converted to Fe^0 when the temperature is higher than 850 °C [30,31].

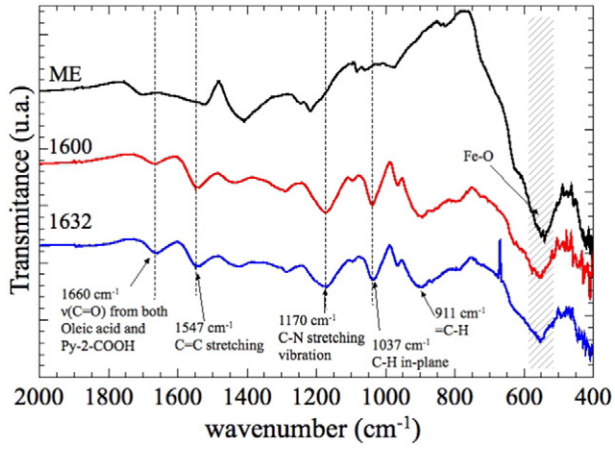

Fig. 3. FTIR spectra of magnetic emulsion (ME), sample 1600 and 1632 in the spectral range of 2000 cm^{-1} to 800 cm^{-1}.

Fig. 4B shows the TGA results of magnetic latexes. In this figure, it could be observed that degradation steps up to 800 °C overlapping each other, then it was difficult to estimate the exact polymer contents. In addition, it is important to point out the presence of a new degradation step (between 400–760 °C) for samples 1608, 1616, 1632, and 3232. This difference on the degradation step may be associated with the presence of Py-2-COOH copolymerized on the particle shell. The same thermal behavior is observed for samples 1616-PVP0, 1616-PVP5, and 1616-PVP10 (see Supplementary data).

When degradation temperature is higher than 850 °C the residual mass became constant indicating that organic parts (oleic acid, polymers, and surfactants) were completely removed and the iron content on each sample could be estimated, as shown in Table 2. For all samples, the percentages in weight (wt.%) were in between 45–52%. These values are very close; indicating that the percentage of iron encapsulated was not affected by the used recipe.

4.5. Magnetic properties

Magnetic curves for the dried latexes obtained by seeded polymerization are presented in Fig. 5. According to the results, all the samples showed superparamagnetic characteristics at room temperature. The saturation magnetization (SM) for magnetic emulsion was 41.54 emu g^{-1} while, for all samples, SM values were between 29 emu g^{-1} and 36 emu g^{-1}. Magnetic content was calculated by the following equation:

$$\textit{Magnetic content} = \frac{MS}{MS_0} \times 100 \quad (1)$$

where MS is the saturation magnetization of dry magnetic latex particles, and MS_0 is the saturation magnetization of dry magnetic emulsion [32]. The results are shown in Table 2. The samples showed magnetic contents higher than 80 wt.% (except for sample 1600). However, both the magnetic properties and the magnetic contents were not dependent of the experimental conditions.

According to papers published elsewhere, saturation magnetization (SM) of iron oxide can be found between 60 emu g^{-1} and 80 emu g^{-1} depending on the predominant crystalline phase [19,22,33]. In our work, oil in water magnetic emulsion (ME) was used. The magnetic emulsion is obtained dispersing iron oxide in octane followed by dispersion in water using surfactants (i.e. SDS). Therefore, magnetic emulsion has a significant percentage of non-magnetic material on its composition, which, in turn, contributes to decrease saturation magnetization to 41.54 emu g^{-1}. In this work, magnetic emulsion was used as the seed during polymerization. Thus its saturation magnetization value was used as reference. For core–shell particles, the percentage of non-magnetic material was increased after coating magnetic emulsion with poly(pyrrole-co-pyrrole-2-carboxylic acid). As a consequence,

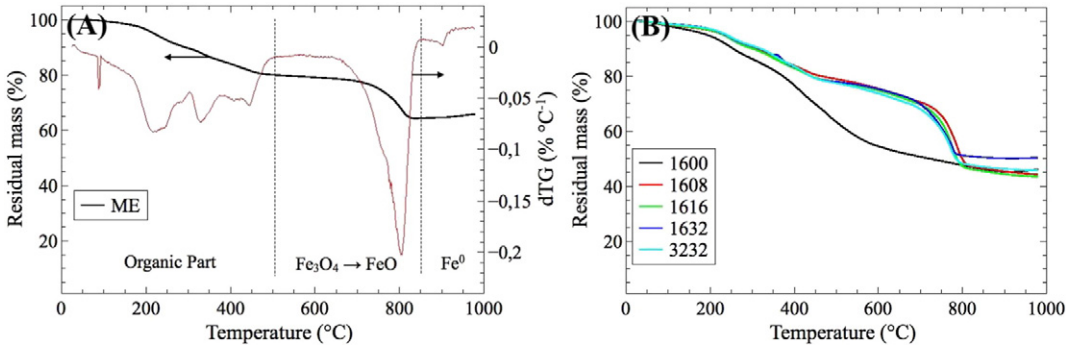

Fig. 4. Thermogravimetric curves of dried samples. (A) TGA and dTG of the magnetic emulsion seed, (B) TGA of magnetic latexes.

saturation magnetization of core–shell particles decreases as can be observed in Fig. 5. However, if compared to the reference sample, saturation magnetization values of core–shell particles decreased slightly indicating the presence of a thin polymeric external layer with a huge amount of magnetic material in their core.

4.6. Particle size

For samples 1600, 1608, 1616, and 3232 the average size was in between 270–295 nm. However, when the amount of Py-2-COOH was increase two times, if compared to 1616, sample 1632 showed an average size of 672 nm. The reason of this high value in size may be associated with particle agglomeration during the earlier stages of polymerization. The carbonyl groups from Py-2-COOH present on the Fe_3O_4 surface may interact with other iron oxide particles favoring particle agglomeration.

The effect of PVP (stabilizer) on the particle size was also investigated. It can be seen in Table 2 that final particle size decreased from 583 nm to 277 nm when the amount of PVP was increased from 0 to 20 mg evidencing the role of stabilizer during the synthesis.

4.7. Cyclic voltammetry (CV)

In order to have an insight about the sample conductivity, the core–shell particles were electrochemically deposited on gold substrate using CV technique. For each sample of magnetic dispersion, a new gold working electrode was used. The window of potential for electrodeposition was from −0.4 V to 0.6 V with a scan rate of 100 mV s^{-1}. While CV technique was applied from −0.3 to 0.5 V with a scan rate of 100 mV s^{-1}.

Fig. 6 shows the CV characterization of conducting magnetic particles (CMP) obtained after electrodeposition on bare gold (BG). Electrodes containing particles showed a single electron oxidation-process similar to bare gold. Cathodic and anodic peaks were respectively 0.1 and 0.3 V vs SCE. It can be seen in Fig. 6A that the peak current of BG containing magnetic particles changed with monomer composition. As shown in Fig. 6A, the peak current increased with the increase of pyrrole concentration (samples 1600, 1608, and 1616). However, a contrary effect was observed when the amount of Py-2-COOH increased. This behavior may be associated with the influence of carboxylic amount on the particle surface. In fact, when Py-2-COOH was used in high concentrations, electron transfer was hindered.

Fig. 6B shows cyclic voltammetry characterization of BG after electrodeposition of conducting magnetic particles changing PVP amount. In this case, except for sample 1616-PVP5, no significant variation in the peak current by addition of PVP during particle preparation was observed.

Table 2
Particle size, iron oxide content, and magnetic content of the obtained particles.

Sample name	Particle size (nm)	Iron content (wt.%)[a]	Magnetic content (wt.%)[c]
ME	193 ± 5	65.8	ND
1600	276 ± 25	45.0	72.1
1608	294 ± 24	45.3	95.1
1616	277 ± 33	44.3	92.7
1632	672 ± 125[b]	50.1	86.3
3232	283 ± 9	46.2	82.3
1616-PVP0	583 ± 217[b]	50.0	ND
1616-PVP5	404 ± 48[b]	50.6	ND
1616-PVP10	327 ± 37[b]	51.1	ND

ND: not determined.
[a] Determined by TGA.
[b] Particle agglomeration.
[c] Determined by magnetization.

4.8. Impedance spectroscopy

Impedance spectroscopy analyses (Fig. 7) were performed after each electrodeposition of different samples. The applied potential at the WE was 0.228 V within a window of frequency from 100 mHZ to 200 kHz. As it was mentioned in the cyclic voltammetry part, the conductivity of the WE surface has increased (decrease of impedance) after MNP deposition for samples: 1600, 1608 and 1616, which can be correlated to the high conductivity of PPy. By increasing the Py-2-COOH concentration (sample 1632), the impedance has increased thus highlighting a deposition of an insulating layer onto the WE surface, which is in agreement with CV characterization after MNP electrodeposition. The same behavior of impedance was also seen for sample 3232 even when the concentration of Ppy was increased from 16 mmol (sample 1632) to 32 mmol (sample 3232). This was due to the high concentration of carboxylic acid amount, which may affect the polymerization of Ppy during the synthesis process of MNP, thus allowing a decrease of the electrical signal of WE after magnetic particle deposition.

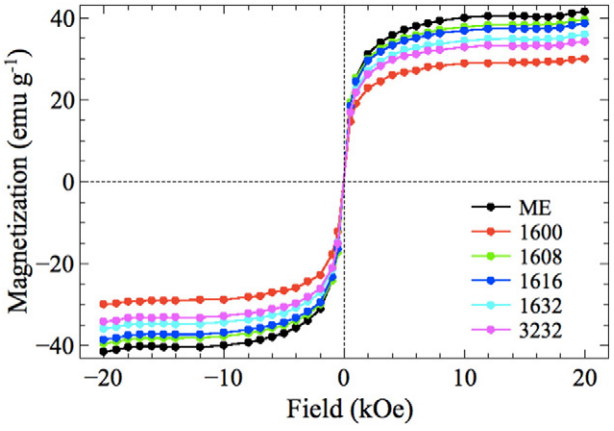

Fig. 5. Magnetization curves of superparamagnetic polymeric particles obtained by seeded polymerization with different Py and Py-2-COOH contents

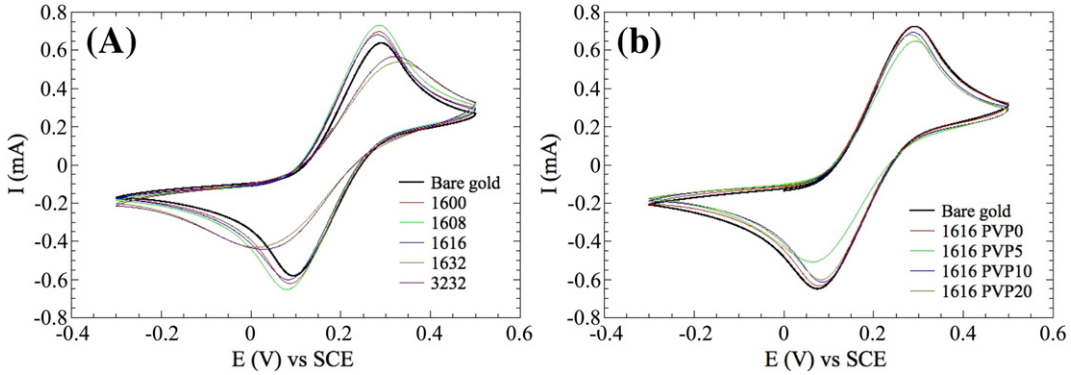

Fig. 6. CV characterization after electrodeposition of conducting magnetic particles: (A) Changing monomers composition, and (B) changing PVP amount.

5. Conclusions

Conducting magnetic particles were successfully synthesized by a simple chemical route. The resulting magnetic core-conducting polymer shell has both ferromagnetic and electric properties as shown by magnetization, cyclic voltammetry and impedance spectroscopy analysis results. Properties of the obtained material can be adjusted by changing Py-2-COOH initial concentration during polymerization. Neither final morphology nor electric properties were changed by the presence of a stabilizing agent (PVP). However, the use of PVP during the synthesis is important to control the colloidal stability and also the shell morphology as shown via size measurements and TEM analysis. The prepared magnetic particles showed conducting property and superparamagnetic behavior, which is important for fast separation under magnetic field when used for sample preparation for instance. In addition, due to the presence of Py-2-COOH in the polymer shell, covalent coupling of amine containing biomolecules (oligonucleotides, proteins, and antibodies, specific ligands) will be possible and for sensors and lab-on-a-chip, microsystems, and microfluidic use.

Acknowledgments

We acknowledge the funding through the projects NATO (CBP.NUKR.SFR 984173), SEA-on-a-CHIP (FP7-2007-013) under the grant agreement no. 248763, the European Union's Horizon 2020 research and innovation program entitled HEARTEN (No 643694), and the fellowship from Science Without Borders program — Conselho Nacional de Desenvolvimento Científico e Tecnológico (CNPq) — Brazil (249056/2013-5).

Appendix A. Supplementary data

Supplementary data to this article can be found online at http://dx.doi.org/10.1016/j.msec.2015.12.052.

References

[1] H. Yoon, Nanomaterials 3 (2013) 524–549, http://dx.doi.org/10.3390/nano3030524.
[2] N. Wang, G. Li, Z. Yu, X. Zhang, X. Qi, Carbohydr. Polym. 127 (20) (2015) 332–339, http://dx.doi.org/10.1016/j.carbpol.2015.03.076.
[3] H. Yoon, J. Jang, Adv. Funct. Mater. 19 (2009) 1567–1576, http://dx.doi.org/10.1002/adfm.200801141.
[4] L.M. Castano, A.B. Flatau, Smart Mater. Struct. 23 (5) (2014), 053001http://dx.doi.org/10.1088/0964-1726/23/5/053001.
[5] Z. Shahnavaz, F. Lorestani, Y. Alias, P.M. Woi, Appl. Surf. Sci. 317 (2014) 622–629, http://dx.doi.org/10.1016/j.apsusc.2014.08.194.
[6] K.S. Jang, H. Lee, B. Moon, Synth. Met. 143 (3) (2004) 289–294, http://dx.doi.org/10.1016/j.synthmet.2003.12.013.
[7] P. Montoya, S. Mejía, V.R. Gonçales, S.I.C. de Torresi, J.A. Calderón, Sensors Actuators B Chem. 213 (2015) 444–451, http://dx.doi.org/10.1016/j.snb.2015.02.118.
[8] M.M. Rahman, X.B. Li, N.S. Lopa, S.J. Ahn, J.J. Lee, Sensors 15 (2) (2015) 3801–3829, http://dx.doi.org/10.3390/s150203801.
[9] M. Lin, M.S. Cho, W.S. Choe, Y. Lee, Biosens. Bioelectron. 25 (1) (2009) 28–33, http://dx.doi.org/10.1016/j.bios.2009.05.035.
[10] N. Pimpha, S. Chaleawlert-umpon, P. Sunintaboon, Polymer 53 (10) (2012) 2015–2022, http://dx.doi.org/10.1016/j.polymer.2012.03.019.
[11] H. Liu, C. Wang, Q. Gao, X. Liu, Z. Tong, Acta Biomater. 6 (2010) 275–281, http://dx.doi.org/10.1016/j.actbio.2009.06.018.
[12] S. Chakraborty, K. Jähnichen, H. Komber, A.A. Basfar, B. Voit, Macromolecules 47 (2014) 4186–4198, http://dx.doi.org/10.1021/ma5008013.
[13] D. Horak, M. Trchova, M.J. Benes, M. Veverka, E. Pollert, Polymer 51 (2010) 3116–3122, http://dx.doi.org/10.1016/j.polymer.2010.04.055.
[14] R.A. Ramli, W.A. Laftah, S. Hashim, RSC Adv. 3 (2013) 15543–15565, http://dx.doi.org/10.1039/C3RA41296B.
[15] A.P. Romio, H.H. Rodrigues, A. Peres, A. Da Cas Viegas, E. Kobitskaya, U. Ziener, K. Landfester, C. Sayer, P.H.H. Araujo, J. Appl. Polym. Sci. 129 (2013) 1426–1433, http://dx.doi.org/10.1002/app.38840.

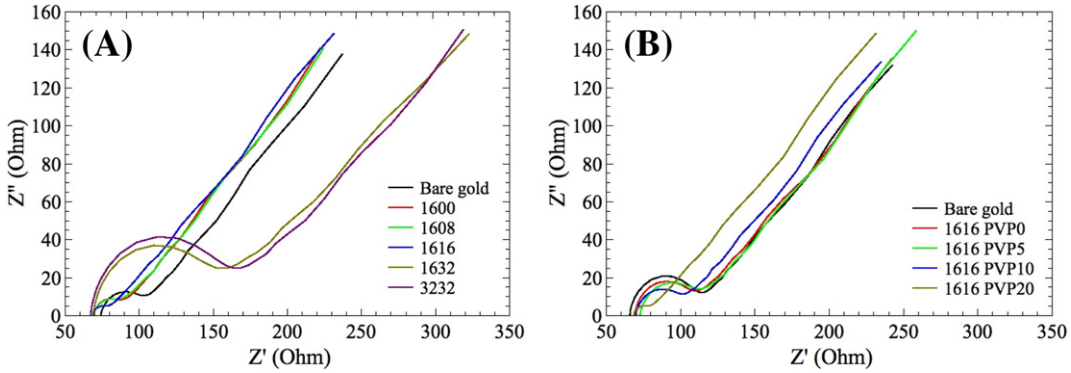

Fig. 7. Impedance spectroscopy analysis before and after electrodeposition of modified MNP for different sample compositions: (A) Changing monomers composition, and (B) changing PVP amount.

[16] J. Ugelstad, Ø. Olsvik, R. Schmid, A. Berge, S. Funderud, K. Nustad, in: T. Ngo (Ed.), in Molecular Interactions in Bioseparations, Springer, US 1993, p. 229.
[17] F. Montagne, O. Mondain-Monval, C. Pichot, Elaissari, A, J. Polym. Sci. A Polym. Chem. 44 (8) (2006) 2642–2656, http://dx.doi.org/10.1002/pola.21391.
[18] M.M. Rahman, M.M. Chehimi, A. Elaissari, J. Colloid Sci. Biotechnol. 3 (2014) 46–57, http://dx.doi.org/10.1166/jcsb.2014.1075.
[19] L.Q. Xie, S.H. Ma, Q. Yang, F. Lan, Y. Wu, Z.W. Gu, RSC Adv. 4 (2014) 1055–1061, http://dx.doi.org/10.1039/C3RA44640A.
[20] R.X. Gao, X.R. Mu, J.J. Zhang, Y.H. Tang, J. Mater. Chem. B 2 (2014) 783–792, http://dx.doi.org/10.1039/C3TB21424A.
[21] N. Naseer, H. Fatima, A. Asghar, N. Fatima, N. Ahmed, A.U. Khan, N.M. Ahmad, J. Colloid Sci. Biotechnol. 3 (2014) 19–29, http://dx.doi.org/10.1166/jcsb.2014.1073.
[22] M.M. Eissa, M.M. Rahman, N. Zine, N. Jaffrezic, A. Errachid, H. Fessi, A. Elaissari, Acta Biomater. 9 (2013) 5573–5582, http://dx.doi.org/10.1016/j.actbio.2012.10.027.
[23] H. Agha, J.-B. Fleury, Y. Galerne, Colloids Surf. A Physicochem. Eng. Asp. 462 (2014) 217–224, http://dx.doi.org/10.1016/j.colsurfa.2014.09.016.
[24] M. Bloemen, W. Brullot, T.T. Luong, N. Geukens, A. Gils, T. Verbiest, J. Nanoparticle Res. 14 (2012) 1100–1110, http://dx.doi.org/10.1007/s11051-012-1100-5.
[25] L. Zhang, R. He, H.-C. Gu, Appl. Surf. Sci. 253 (5) (2006) 2611–2617, http://dx.doi.org/10.1016/j.apsusc.2006.05.023.
[26] R.M. Silverstein, F.X. Webster, D. Kiemle, Spectrometric Identification of Organic Compounds, seventh ed. Wiley Global Education, 2005.
[27] A.T. Dubis, S.J. Grabowski, D.B. Romanowska, T. Misiaszek, J. Leszczynski, J. Phys. Chem. A 106 (2002) 10613–10621, http://dx.doi.org/10.1021/jp0211786.
[28] J. Upadhyay, A. Kumar, B. Gogoi, A.K. Buragohain, Mater. Sci. Eng. C 54 (2015) 8–13, http://dx.doi.org/10.1016/j.msec.2015.04.027.
[29] Z. Yang, X. Shang, C. Zhang, J. Zhu, Sensors Actuators B Chem. 201 (2014) 167–172, http://dx.doi.org/10.1016/j.snb.2014.05.021.
[30] M. Mahdavi, M.B. Ahmad, M.J. Haron, F. Namvar, B. Nadi, M.Z.A. Rahman, J. Amin, Molecules 18 (7) (2013) 7533–7548, http://dx.doi.org/10.3390/molecules18077533.
[31] S.Y. Zhao, K.L. Don, W.K. Chang, G.C. Hyun, H.K. Young, S.K. Young, Bull. Kor. Chem. Soc. 27 (2) (2006) 237–242, http://dx.doi.org/10.5012/bkcs.2006.27.2.237.
[32] E.T. Tenório-Neto, T. Jamshaid, M. Eissa, M.H. Kunita, N. Zine, G. Augusti, H. Fessi, A.E. El-Salhi, A. Elaissari, Polym. Adv. Technol. 26 (2015) 1199–1208, http://dx.doi.org/10.1002/pat.3562.
[33] P. Kucheryavy, J. He, V.T. John, P. Maharjan, L. Spinu, G.Z. Goloverda, V.L. Kolesnichenko, Langmuir 29 (2013) 710–716, http://dx.doi.org/10.1021/la3037007.